Toxicology Letters 181 (2008) 104–111

Contents lists available at ScienceDirect

Toxicology Letters

journal homepage: www.elsevier.com/locate/toxlet

Effects of 3-benzidino-6-phenylpyridazine, as an acetylcholinesterase inhibitor, on outward potassium current in acutely isolated rat hippocampal pyramidal neurons

Huizhi Du, Miaoyu Li, Pin Yang*

Institute of Molecular Science, Key Laboratory of Chemical Biology and Molecular Engineering of Ministry of Education, Shanxi University, Wucheng Road 92, Taiyuan 030006, PR China

ARTICLE INFO

Article history:
Received 21 March 2008
Received in revised form 3 July 2008
Accepted 4 July 2008
Available online 15 July 2008

Keywords:
Whole cell patch-clamp technique
Hippocampal pyramidal neurons
3-Benzidino-6-phenylpyridazine
Outward potassium currents
Electric eel acetylcholinesterase

ABSTRACT

As an acetylcholinesterase (AChE) inhibitor, the effects of 3-benzidino-6-phenylpyridazine (BPP) on outward potassium current including delayed rectifier potassium current ($I_{K(DR)}$) and transient outward potassium current ($I_{K(A)}$) in acutely isolated rat hippocampal pyramidal neurons were studied, using the whole cell patch-clamp technique. BPP reversibly inhibited electric eel AChE as an inhibitor, with IC_{50} of 1.43 μM. BPP (0.10–100 μM) decreased $I_{K(DR)}$ and $I_{K(A)}$ in a concentration-dependent, voltage-independent and partial reversible manner, with IC_{50} of 0.47 and 0.31 μM, respectively. 10 μM BPP did not affect steady-state activation of $I_{K(DR)}$ and $I_{K(A)}$. In addition, 10 μM BPP shifted the voltage dependence of steady-state inactivation of $I_{K(A)}$ towards negative potential. In conclusion, BPP potently inhibits $I_{K(DR)}$ and $I_{K(A)}$ in rat hippocampal pyramidal neurons, which may contribute to BPP's restoring the damaged central nervous system.

1. Introduction

Alzheimer's disease (AD), the most common cause of dementia in the elderly, is a chronic, slowly progressive neurodegenerative disorder with characteristic deterioration of intellectual capacity in various domains: learning and memory, language abilities, reading and writing, praxis, interaction with the environment (Tariot, 1994). It was hypothesized that the cognitive loss associated with AD was related to reduction of acetylcholine (ACh) and central cholinergic deficit. Thus, increasing ACh amounts by acetylcholinesterase (AChE) inhibitors might enhance cognitive function in AD patients (Benzi and Moretti, 1998; Mega, 2000). So far, many kinds of AChE inhibitors, such as tetrahydroaminoacridine (tacrine) and galantamine have been exploited and applied (Sugimoto, 1999). Hippocampal neurons are the most important region for learning and memory in brain. Biological membranes are essential in maintaining cell integrity and function. Ion channels in cell membrane are targets for many toxins and drugs. Much medical damage or mend to the central nervous system (CNS) is achieved through medical disturbance of the function of ion channels (Calavresi et al., 1995; Taylor and Meldrum, 1995). There are many kinds of ion channels in rat hippocampal neurons, such as potassium channels, calcium channels and sodium channels, etc. Potassium channels are primarily responsible for the depolarization phase of the action potential (Müller and Misgeld, 1990, 1991). They play important roles in regulation of learning and memory (Harvey and Rowan, 1990; Landifield and Pilter, 1984) and the electrical excitability of animal cells. Enhancement of outward potassium current may participate in cortical neuronal death in AD (Yu et al., 1998). Several AChE inhibitors have been found effective on outward potassium currents. Tacrine inhibits delayed rectifier potassium current ($I_{K(DR)}$) (Kraliz and Singh, 1997; Zhang et al., 2004) and transient outward potassium current ($I_{K(A)}$) (Rogawski, 1987). Metrifonate inhibits slow component of the afterhyperpolarization tail current (sI_{AHP}) (Power et al., 2001). Galantamine blocks $I_{K(DR)}$, but not $I_{K(A)}$ in rat dissociated hippocampal pyramidal neurons (Pan et al., 2002). Donepezil blocks $I_{K(DR)}$ in pyramidal neurons of rat hippocampus and neocortex (Zhong et al., 2002).

3-[(β-Morpholinoethyl)amino]-4-methyl-6-phenylpyridazine (minaprine, Fig. 1) has selective affinity for muscarinc M_1 receptors and possesses related memory-enhancing properties (Sansone et al., 1995; Worms et al., 1989). Also, it enhances short-term retention in rats in the social memory test (Puglisi-Allegra et al., 1994). Thus, minaprine may be developed into a potential remedy for the treatment of senile dementias and cognitive impairments occurring in elderly people. Because a classical structure–activity

* Corresponding author.
E-mail address: yangpin070705@sina.com (P. Yang).

0378-4274/$ – see front matter © 2008 Elsevier Ireland Ltd. All rights reserved.
doi:10.1016/j.toxlet.2008.07.004

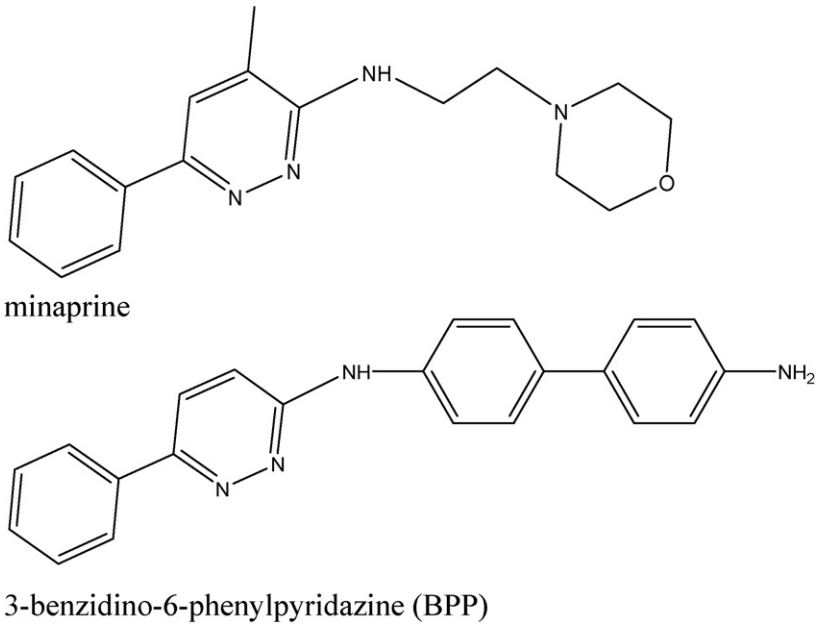

Fig. 1. Structures of minaprine and 3-benzidino-6-phenylpyridazine (BPP).

relationship exploration suggests that the critical elements for high AChE inhibition be as follows: (i) presence of a central pyridazine ring, (ii) necessity of a lipophilic cationic head, (iii) change from a 2- to a 4–5-carbon unit distance between the pyridazine ring and the cationic head (Contreras et al., 1999). Using pyridazine and benzidine as building blocks, we firstly synthesized 3-benzidino-6(4-chlorophenyl) pyridazine (BCP), 3-benzidino-6-phenylpyridazine (BPP) in our laboratory. These compounds and minaprine have a central pyridazine ring in common. We have found that BCP potently inhibits $I_{K(DR)}$ and $I_{K(A)}$ in a concentration-dependent and voltage-dependent manner in acutely isolated rat hippocampal pyramidal neurons by using whole cell patch-clamp technique, besides inhibiting electric eel AChE (Du et al., 2006). In the present study, we investigated the effects of BPP on electric eel AChE and two main voltage-activated outward potassium currents including $I_{K(DR)}$ and $I_{K(A)}$ in acutely isolated rat hippocampal pyramidal neurons.

2. Materials and methods

2.1. Assay of electric eel AChE activities in vitro

Firstly, we selected a suitable concentration of AChE, at which the relationship between the initial velocity and the concentration of AChE ([AChE]) should be linear (Chen and Zhou, 2001; Kamal et al., 2000). Secondly, AChE activity was measured, using acetylthiocholine iodide (ASCh) as the substrate of the enzymatic reaction and 5,5′-dithio-bis (2-nitrobenzoic acid) (DTNB) as the chromogenic agent (Ellman et al., 1961). 0.31–9.38 Units/ml of AChE was assayed in the buffer solution in vitro from 30 s–10 min, at room temperature. The change of rate of substrate cleavage was determined by measuring the absorbance of the reaction product at 412 nm wavelength.

AChE solution (1.56 Units/ml), DTNB (20.33 mM) and ASCh (30.28 mM) in assay buffer was stored at 4 °C. 2430 μl of assay buffer, 25 μl of AChE solution and 20 μl of BPP solutions were mixed. After 10 min of preincubation at 37 °C, 2000 μl of the mixture was moved into a cuvette. And then, 25 μl of DTNB and 20 μl of ASCh were successively added to the mixture. After 1 min, the change in absorbance at 412 nm was recorded on a HP-8453 spectrophotometer.

2.2. Isolation of single rat hippocampal pyramidal neurons

Single rat hippocampal pyramidal neurons were acutely isolated by enzymatic digestion and mechanical dispersion (Du et al., 2006). Wistar rats of 7–10 days were purchased from the Experimental Animal Center of Shanxi Medical University (Grade II, Certificate No. 070101). All experiments conformed to local and international guidelines on ethical use of animals and all efforts were made to minimize the number of animal used and suffering. Briefly, 400–600 μm thick brain slices were cut from hippocampal region in ice-cold artificial cerebrospinal solution (ACS). These tissue pieces were incubated for at least 30 min at 32 °C in ACS, and then transferred into ACS containing 0.5 mg/ml protease at 32 °C for 35 min. Throughout the entire procedure the media were continuously saturated with a 95% O_2–5% CO_2 gas to maintain a pH value as 7.40. After digestion, the tissue pieces were washed 3 times with ACS. Through a series of Pasteur pipettes with decreasing tip diameter, neurons were isolated by triturating the brain fragments. Then, the cell suspension was maintained at room temperature in extracellular solution, and was ready for the electrophysiological experiment. All experiments were performed within 4 h after isolation.

2.3. Patch-clamp recording technique

The cell suspension was transferred into an experimental chamber mounted on the stage of an inverted microscope (Chongqing, China) with 1 ml extracellular solution. After 20 min, pyramidal cells settled on the bottom of the chamber. $I_{K(DR)}$ and $I_{K(A)}$ currents were recorded with an Axopatch 200B patch-clamp amplifier (Axon Instruments, Foster City, CA, USA). Glass microelectrodes were made using micropipette puller (PP 830, Narishige, Japan) and had a resistance of 7–12 MΩ when filled with electrode internal solution. Neurons with bright, smooth appearance and apical dendrites were selected for recording. Liquid junction potential between the pipette solution and external solution was corrected after the pipette tipped into the external solution. After forming a conventional "gigaseal", the membrane was ruptured with a gentle suction to obtain the whole cell voltage clamp. To minimize the duration of capacitive current, membrane capacitance and series resistance were compensated after membrane rupture. Evoked currents were low-pass filtered at 2 kHz, digitized at 10 kHz, command pulses were generated by a Digidata 1200B (Axon) controlled by pCLAMP version 6.0.4 software (Axon Instruments, CA, USA), and on-line acquired data stored in a PC486 computer for subsequent analysis. All experiments were carried out at room temperature (20–26 °C).

2.4. Solutions

Assay buffer was 100 mM phosphate buffer solution, pH 7.20. The buffer solution contained (in mM): ASCh 22.48 and DTNB 20.19 in assay buffer.

Artificial cerebrospinal solution (ACS) contained (in mM): NaCl 124, KCl 5, KH_2PO_4 1.20, $MgSO_4$ 1.30, $CaCl_2$ 2.40, Glucose 10, $NaHCO_3$ 26, pH 7.40. External solution contained (in mM): NaCl 150, KCl 5, $MgCl_2$ 1.10, $CaCl_2$ 2.60, Glucose 10, HEPES 10, TTX 0.001, $CdCl_2$ 0.20, pH 7.40. Electrode internal solution contained (in mM): KCl 65, KOH 5, KF 80, $MgCl_2$ 2, HEPES 10, EGTA 10, Na_2ATP 2, pH 7.30.

2.5. Data analysis

All data were analyzed by the use of pCLAMP 6.0 and Origin 5.0 software (Microcal software, USA). All values were presented as mean ± S.D., and statistical

comparisons were made using the paired Student's *t* test and one-way ANOVA procedure, and the probabilities less than 0.05 were considered significant.

3. Results

3.1. The effects of BPP on electric eel AChE

3.1.1. Choice of assay conditions

The data shown in Fig. 2 were used to determine the limits of linearity with regard to absorbance versus reaction time for different [AChE]. The response was not linear for any except 0.31–1.56 Units/ml. However, it can be seen that the value of absorbance is on the linear increase up to time of 3 min for different [AChE] (Fig. 2A). The initial reaction velocities of each amount of AChE at 0–3 and 0–10 min were plotted against [AChE] (Fig. 2B). The correlation coefficient (*R*) was 0.9993 for all of [AChE] at 0–3 min, and 0.9985 for 0.31–6.25 Units/ml of [AChE] at 0–10 min. As a consequence, a concentration of not surpassing 0.04 Units/ml of AChE and the initial velocity of 0–3 min were chosen as suitable conditions in further studies.

3.1.2. Determination of inhibitory potency

Firstly, the initial velocities (0–3 min) were obtained by the method of 2.1 in Section 2. The percent inhibition of BPP in different concentrations (0.14, 0.19, 0.28, 1.40 and 2.80 μM) was calculated from the initial velocities. Inhibition curves were obtained by plotting the percent inhibition versus the logarithm of BPP concentration (Fig. 3A). The results show that BPP inhibit electric eel AChE activity in a concentration-dependent manner, and IC_{50} value (50% of maximum inhibition) is 1.43 μM, with *R* of 0.9987.

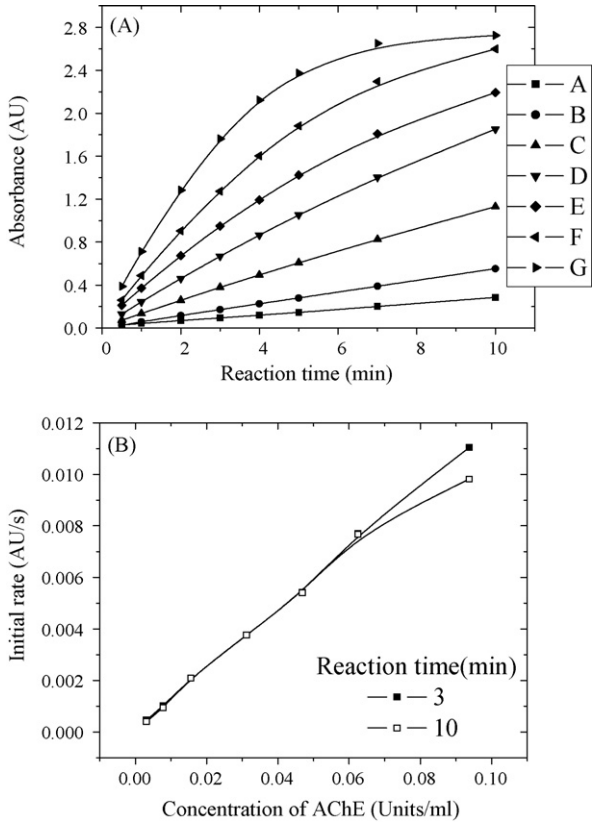

Fig. 2. Assay of acetylcholinesterase (AChE) activities. (A) Absorbance as a function of time at different concentrations of AChE ([AChE]) as indicated in legend box. [AChE] are 0.31, 0.78, 1.56, 3.13, 4.69, 6.25 and 9.38 Units/ml from A to G, respectively. (B) Initial velocity as a function of [AChE]. The correlation coefficient (*R*) was 0.9993 for all of [AChE] at 0–3 min, and *R* was 0.9985 for 0.31–6.25 Units/ml of [AChE] at 0–10 min.

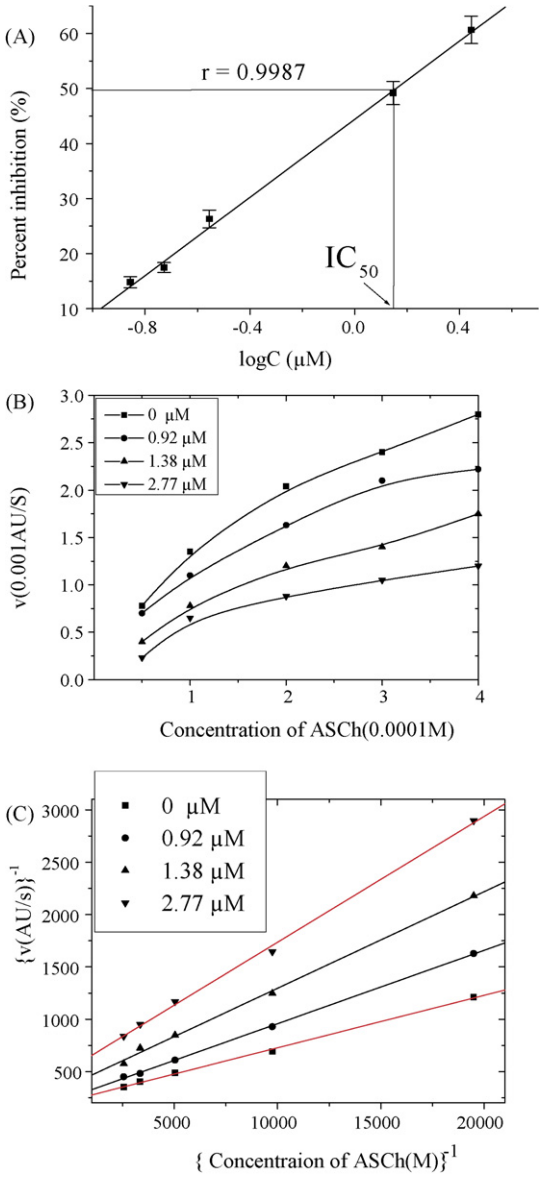

Fig. 3. The effects of BPP on electric eel AChE. (A) Concentration–response curve of effect of BPP on electric ell AChE. IC_{50} value is 1.43 μM, with *R* of 0.9987. (B) Plots representing initial velocity of AChE versus ASCh concentration in the absence and presence of different concentrations of BPP (0, 0.92, 1.38 and 2.77 μM, respectively). (C) Linweaver-Burk plots representing the reciprocal of initial velocity of AChE versus the reciprocal of ASCh concentration in the absence and presence of different concentrations of BPP. *R* was 0.9992, 0.9998, 0.9989 and 0.9991 for different concentrations of BPP (0, 0.92, 1.38 and 2.77 μM, respectively).

Upon the application of BPP, the initial velocity decreased gradually; when the concentration of BPP remained the same, the reduced concentration of the substrate (ASCh) will make it possible that the initial velocity also decreased gradually (Fig. 3B); Fig. 3C indicates that intersections on the ordinate and the slopes of the lines are increasing with higher concentration of BPP (0, 0.92, 1.38, 2.77 μM). Therefore, it can be inferred that the nature of the inhibition by BPP was the partial non-competitive type. In addition, we could obtain its related K_{mapp} (K_m) and V_{maxapp} (V_{max}) from the intersections of the abscissa and the ordinate (Table 1).

Table 1
The effects of BPP on K_m and V_{max} of electric eel AChE

Concentration of BPP (μM)	K_m (mM)	V_{max} (mAU/S)
0	0.22	4.35
0.92	0.27	3.89
1.38	0.25	2.68
2.77	0.22	1.87

3.2. The effects of BPP on $I_{K(DR)}$ and $I_{K(A)}$

3.2.1. Separation of $I_{K(DR)}$ and $I_{K(A)}$

In whole cell patch-clamp recording, the total potassium currents were recorded with 150 ms depolarizing pulses from −50 to +60 mV in 10 mV steps following a hyperpolarizing prepulse of 400 ms to −110 mV (Fig. 4A). The delayed rectifier potassium currents ($I_{K(DR)}$) were elicited by a similar protocol in which a 50 ms interval at −50 mV was inserted after the prepulse. Currents at the end of the depolarizing pulse were referred to as $I_{K(DR)}$ (Fig. 4B). Subtraction of Fig. 4B from Fig. 4A revealed the fast transient potassium currents ($I_{K(A)}$). The peak of the subtracted currents was referred to as $I_{K(A)}$ (Fig. 4C).

The effects of BPP on $I_{K(DR)}$ and $I_{K(A)}$ were observed at +60 mV when depolarized from −50 mV. In the control test without BPP, $I_{K(DR)}$ and $I_{K(A)}$ decreased by 3.50 ± 2.10% and 4.20 ± 3.00% (n = 8) in 15 min current-recording, respectively. Upon the application of BPP, the inhibitory effects occurred in a few minutes until reached a maximum and steady value in about 12 min (data not shown). With different concentration of BPP, it took 12 ± 2 min for inhibitory effects on $I_{K(DR)}$ and $I_{K(A)}$ to reach the steady value. Therefore, in the present study, signals were firstly recorded in natural states, and then recorded in 12 min after addition of BPP into external solution.

3.2.2. BPP decreased $I_{K(DR)}$ and $I_{K(A)}$ in a concentration-dependent manner

Upon the application of BPP, the amplitudes of $I_{K(DR)}$ and $I_{K(A)}$ decreased, and this action progressed with increment in concentrations from 0.10 to 100 μM (including: 0.10, 1, 5, 10, 50 and 100 μM, respectively). After cessation of the drug and washout, $I_{K(DR)}$ and $I_{K(A)}$ recovered by 87% (Fig. 5A and B). Concentration–response curve was obtained by plotting the percent inhibition against the concentration of BPP (Fig. 5C), and the curve was fitted with the Hill function: $I = I_{max}/[1 + (IC_{50}/C)^n]$, where I is the percent inhibition, I_{max} is the maximal percent inhibition, IC_{50} is 50% of maximum inhibition, C is the concentration of BPP, and n is the Hill coefficient. The IC_{50} value of BPP for blocking $I_{K(DR)}$ was calculated as (0.47 ± 0.13) μM with n of (0.45 ± 0.07), and the IC_{50} value of BPP for blocking $I_{K(A)}$ was calculated as (0.31 ± 0.12) μM with n of (0.45 ± 0.09). The result indicated that BPP decreased $I_{K(DR)}$ and $I_{K(A)}$ in a concentration-dependent manner.

3.2.3. The effects of BPP on current–voltage relationships of $I_{K(DR)}$ and $I_{K(A)}$

Fig. 5D E shows current–voltage (I–V) curves of $I_{K(DR)}$ and $I_{K(A)}$ generated by depolarizing steps from a holding potential of −50 to +60 mV with a 10 mV increment, respectively. In the presence of 10 μM BPP, the amplitude of $I_{K(DR)}$ and $I_{K(A)}$ was significantly decreased at the test potentials between −20 and 60 mV, and the amplitudes of $I_{K(DR)}$ and $I_{K(A)}$ decrease differently at different membrane potentials (n = 5). The relationship between the percent inhibition on $I_{K(DR)}$ and $I_{K(A)}$ and the depolarizing potential was linear; and inhibitory effects did not vary with changes of membrane potential from −20 to +60 mV (Fig. 5F), which indicated that the amplitudes of $I_{K(DR)}$ and $I_{K(A)}$ decreased in a voltage-independent manner. The results indicate that BPP does not sense the electric field in the pore.

3.2.4. The effects of BPP on activation of $I_{K(DR)}$ and $I_{K(A)}$

The effects of BPP on activation of $I_{K(DR)}$ and $I_{K(A)}$ were detected by conductance–voltage relationship. $I_{K(DR)}$ and $I_{K(A)}$ was recorded as Fig. 4. The activation curves for $I_{K(DR)}$ and $I_{K(A)}$ in the absence and presence of 10 μM BPP were shown in Fig. 6A and B. Conductance–voltage curves were constructed by plotting G/G_{max} versus membrane potentials, and the curves were fitted by a Boltzmann equation: $G/G_{max} = 1/\{1 + \exp[(V - V_{1/2})/k]\}$, where G is conductance, G_{max} is maximum conductance, V is membrane potential, $V_{1/2}$ is the potential for half-maximal activation, and k is the slope factor; G was calculated by using the equation: $G = I/(V - V_K)$, where I is current amplitude and V_K is the reversal potential. In the absence and presence of 10 μM BPP, the value of $V_{1/2}$ was (4.61 ± 0.90) and (3.66 ± 0.81) mV (n = 5, P > 0.05), with k of (−11.04 ± 0.85) and (−10.75 ± 0.76) mV (n = 5, P > 0.05) for $I_{K(DR)}$; and the value of $V_{1/2}$ was (16.30 ± 0.77) and (15.80 ± 1.12) mV (n = 5, P > 0.05), with k of (−14.77 ± 0.75) and (−13.80 ± 1.09) mV (n = 5, P > 0.05) for $I_{K(A)}$. BPP (10 μM) did not affect the activation curves of $I_{K(DR)}$ and $I_{K(A)}$.

3.2.5. The effects of BPP on steady-state inactivation of $I_{K(A)}$

Fig. 6C shows the effects of BPP on the voltage-dependence of $I_{K(A)}$ inactivation using a double-pulse protocol: currents were

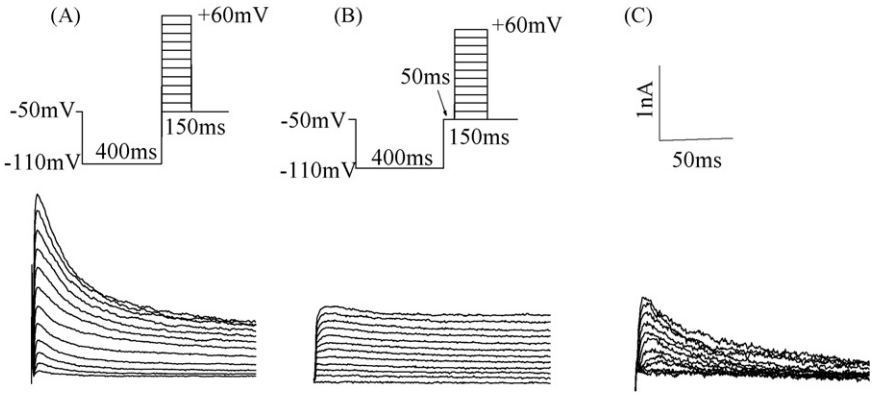

Fig. 4. Outward potassium currents in a hippocampal pyramidal neuron. (A) Total outward potassium currents stimulated with 150 ms depolarizing pulses from −50 to +60 mV in 10 mV steps following a hyperpolarizing prepulse of 400 ms to −110 mV (inset). (B) $I_{K(DR)}$ stimulated with similar protocol as in (A), except for a 50 ms interval at −50 mV was inserted after the prepulse (inset). (C) Isolated $I_{K(A)}$ by subtracting current traces of (B) from those of (A).

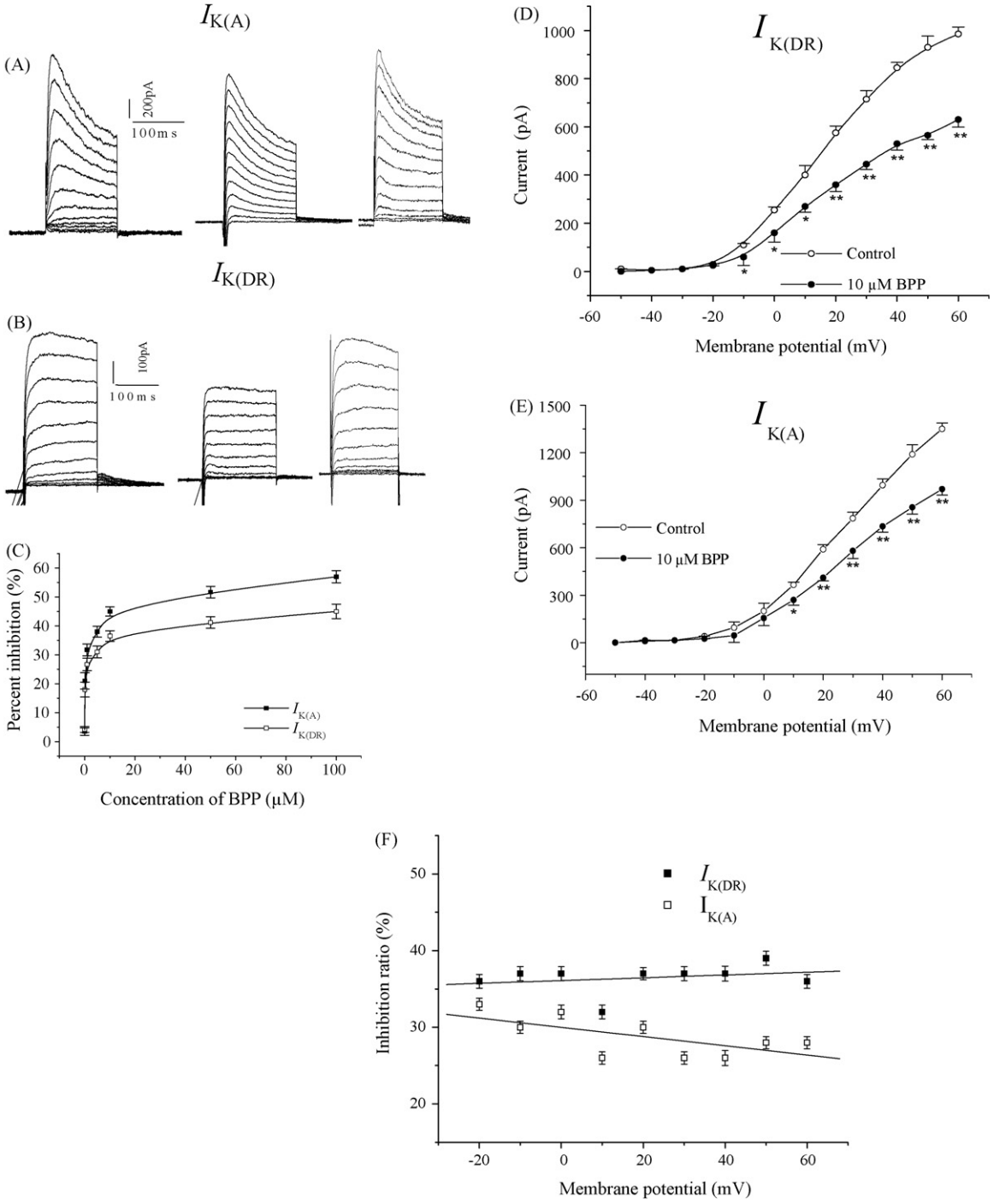

Fig. 5. The effects of BPP on $I_{K(DR)}$ and $I_{K(A)}$. $^{*}P<0.05$, $^{**}P<0.01$ vs. control. (A and B) Current trances of $I_{K(A)}$ and $I_{K(DR)}$ in control (left traces), 10 μM BPP treated (middle traces), and after wash (right trances). (C) Concentration–response curves for the blockade of BPP on $I_{K(DR)}$ and $I_{K(A)}$. Each point represents mean of five cells. (D and E) Current–voltage (I–V) curves of $I_{K(DR)}$ and $I_{K(A)}$ in the absence (○) and presence (●) of 10 μM BPP. Each point represents mean of five cells. (F) Percent inhibition in $I_{K(DR)}$ and $I_{K(A)}$ caused by 10 μM BPP application as a function of depolarizing potentials. The relationship between the percent inhibition on $I_{K(DR)}$ or $I_{K(A)}$ and the depolarizing potential was linear; and inhibitory effects did not vary with changes of membrane potential from −20 to +60 mV. Each point represents mean of five cells.

elicited with a 120 ms test pulse to +60 mV preceded by 80 ms prepulses to potentials between −120 and −10 mV, and holding potential is −100 mV. The inactivation curves were obtained by plotting the normalized $I_{K(A)}$ against the prepulse voltages. The plots were well fitted with a single Boltzmann function: $I/I_{max} = 1/\{1 + \exp[(V - V_{1/2})/k]\}$, where I/I_{max} is the normalized data, V is the prepulse potential, $V_{1/2}$ is the potential where normalized I was reduced to one half and k is the slope factor. In the absence and presence of 10 μM BPP, the value of $V_{1/2}$ was (-21.25 ± 1.13) and (-37.31 ± 1.17) mV ($n = 5$, $P < 0.01$), with k of (-7.87 ± 0.95) and (-7.52 ± 1.02) mV ($n = 5$, $P > 0.05$). BPP (10 μM) caused a negative shift of the inactivation curve along the potential axis. At the same time, the slope factor k remained unchanged.

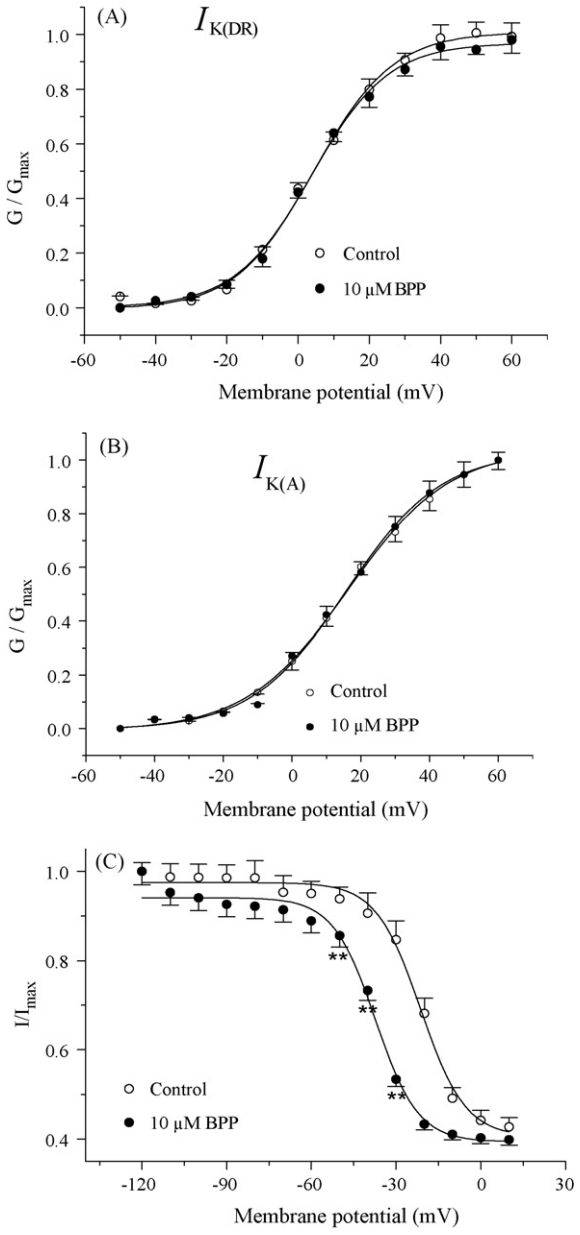

Fig. 6. Normalized steady-state activation and inactivation curves of $I_{K(DR)}$ and $I_{K(A)}$ in the absence (○) and presence (●) of 10 μM BPP were plotted as a function of membrane potential. The curves were fitted with Boltzmann function (see text). The value of each point is mean of five cells. $^{*}P < 0.05$, $^{**}P < 0.01$ vs. control. (A) Steady-state activation curves of $I_{K(DR)}$. (B) Steady-state activation curves of $I_{K(A)}$. (C) Steady-state inactivation curves of $I_{K(A)}$.

4. Discussion

Minaprine, besides its original antidepressive properties, has a character of increasing concentration of AChE that could be, at least in part, mediated by their selective affinity for M1 muscarinic receptors. An *in vivo* administration of minaprine (30 mg/kg) to rats significantly increases ACh levels in the hippocampus (38%). While, minaprine presents a very weak inhibition in vitro on electric eel AChE (IC_{50} = 600 μM) (Contreras et al., 1999; Garattini et al., 1984). Thus, minaprine may be developed into a potential remedy for the treatment of senile dementias and cognitive impairments occurring in elderly people. And, the main acting group of minaprine is pyridazine ring (Worms et al., 1989). Two novel compounds including BCP and BPP have a central pyridazine ring in common with minaprine. We investigated the effects of BCP (Du et al., 2006) and BPP on electric eel AChE, $I_{K(DR)}$ and $I_{K(A)}$ in acutely isolated rat hippocampal pyramidal neurons. In this study, BPP inhibited electric eel AChE as an inhibitor, with IC_{50} of 1.43 μM. The pyridazine and benzidine group of BPP maybe reacts with binding site of the binding pocket in electric eel AChE. In addition, the hydrogen-bonding interaction between BPP and electric eel AChE seems to play an important role (Harel et al., 1993; Sussman et al., 1991; Yamamoto et al., 1994). Plots of the remaining AChE activity versus the concentrations of AChE in the presence of different concentrations of BPP gave a family of straight lines, which all passed through the origin. Increasing the BPP concentration resulted in the descending of the slope of the line, indicating that the inhibition of BPP on the enzyme was reversible reaction course. The presence of BPP did not bring down the amount of the enzyme, but just resulted in the inhibition and the descending of the activity of the enzyme (no listed figures). BPP was reversible inhibitor of electric eel AChE. BPP (0.1–100 μM) decreased $I_{K(DR)}$ and $I_{K(A)}$ in a concentration-dependent and voltage-independent manner, with IC_{50} of 0.47 and 0.31 μM, respectively. It seems that the effects of BPP on $I_{K(A)}$ are slightly more potent than that of BPP on $I_{K(DR)}$. BPP (10 μM) did not affect steady-state activation of $I_{K(DR)}$ and $I_{K(A)}$. In addition, BPP (10 μM) shifted the voltage dependence of steady-state inactivation of $I_{K(A)}$ towards negative potential, and shortened the inactivation time of $I_{K(A)}$. Although, BCP and BPP have a central pyridazine ring in common, the effects of them on electric eel AChE, $I_{K(DR)}$ and $I_{K(A)}$ are not identical. Therefore, the presence of other groups associated with the pyridazine ring might make the compound more specific for either $I_{K(DR)}$ or $I_{K(A)}$. Because two compounds do not make up of a series, some systemization of more new compounds remains in progress and chemical groups combined with pyridazine deserve our considerate attention.

Several AChE inhibitors were found to have effect on outward potassium currents in neurons. However, their effect mechanism was not identical. Tetrahydroaminoacridine (tacrine) inhibits $I_{K(DR)}$ (Kraliz and Singh, 1997; Zhang et al., 2004) and $I_{K(A)}$ (Rogawski, 1987). Galantamine blocks $I_{K(DR)}$, but not $I_{K(A)}$ in rat dissociated hippocampal pyramidal neurons (Pan et al., 2002). Donepezil blocks $I_{K(DR)}$ in pyramidal neurons of rat hippocampus and neocortex (Zhong et al., 2002). These studies differed in three important aspects that displayed in species (mouse vs. rat), cell types (cortical neurons vs. hippocampal neurons) and different approaches to getting cells (cultured cell vs. acutely isolated cell). So the results were not identical. In addition, although tacrine is structurally related to the potassium channel blocker 4-aminopyridine (4-AP), the blockade of potassium channel by tacrine cannot be only attributed to the 4-AP-sensitive $I_{K(A)}$ (Kraliz and Singh, 1997). Further studies involving other pharmacological compounds structurally related to 4-AP or minaprine are needed to understand the role of various groups and structure–activity relationship of AChE inhibitors in the blockade of the potassium current (Sugimoto, 1999).

Under physiological conditions, potassium currents are important for modifying neuronal cellular and network excitability and activity (Müller and Misgeld, 1990, 1991), regulating neuronal excitability and maintaining of baseline membrane potential (Storm, 1990). Potassium channels control action potential duration and repolarization, release of neurotransmitters and hormones, Ca^{2+}-dependent synaptic plasticity (Müller and Bittner, 2002). $I_{K(DR)}$ and $I_{K(A)}$ contribute to action potential repolarization. Since $I_{K(A)}$ is transient, repolarization is mainly related to $I_{K(DR)}$. As in other neurons, $I_{K(A)}$ in hippocampal neurons was thought to modulate the timing of repetitive action potential generation and the time required to reach the threshold to fire an action potential

(Gao and Ziskind-Conhaim, 1998). Enhancement of outward potassium currents leads to a reduction in $[K^+]_i$, which is involved in the pathogenesis of neuronal death (Bortner et al., 1997); also may participate in cortical neuronal death in AD (Yu et al., 1998). In AD rats, a slowly formed transient conformer of $A\beta^{1-40}$ is toxic to inward channels of dissociated hippocampal and cortical neurons (Sun et al., 2003). In our study, BPP inhibited $I_{K(DR)}$ and $I_{K(A)}$ in a concentration-dependent manner, with IC_{50} of 0.47 and 0.31 μM, respectively, which protects the neuron cells from being harmed. But, we also notice that with the increasing of concentration, the effects of suppression of BPP was not so significant and even became stable, and the maximum inhibition on $I_{K(DR)}$ and $I_{K(A)}$ only reaches about 50% even at the maximum concentration of BPP, and the maximal inhibition of BPP on $I_{K(DR)}$ is much stronger than on $I_{K(A)}$. Because voltage-activated K^+ channels in rat pyramidal neurons are composed of various K^+ channel subtypes such as Kv1, Kv2, Kv3 and Kv4, these compounds are probably selective to some K^+ channel subtypes (Pan et al., 2002; Martina et al., 1998). It needs further studies to understand the channel selectivity of these compounds. In addition, the voltage-dependent K^+ currents, Ca^{2+}-dependent K^+ currents activated by depolarization have also been demonstrated in hippocampal neurons (Segal and Barker, 1986).

The mechanism by which AChE inhibitors affect hippocampal potassium channels are not fully understood at this time. However, there are several potential interpretations. One possibility is the electrostatic interactions between BPP and potassium channel proteins. In our study, BPP (10 μM) decreased the amplitudes of $I_{K(DR)}$ and $I_{K(A)}$ in voltage-independent manner, namely, the fractional reduction in $I_{K(DR)}$ and $I_{K(A)}$ upon BPP application was unaffected by changes in the depolarizing potential, indicating that BPP does not sense the electric field in the pore, coming in the vicinity of the selectivity filter of potassium channel. Therefore, if BPP blocks outward potassium channels via binding to channel proteins, it likely binds to an external site rather than inserting into the pore. Furthermore, the inhibition effects of BPP on outward potassium currents were obvious only at potentials more positive than 0 mV. These effects could be attributed to electrostatic interaction of BPP with the membrane (Zhang and Yang, 2006). Another possible mechanism might involve changes in membrane fluidity. Previous studies have indicated that membrane fluidity is altered in central and peripheral cell systems in AD (Hajimohammadreza et al., 1990). BPP seems to have more pronounced effects on membrane integrity and fluidity, which invests BPP with the property of protecting neuron. Because BMP also inhibited $I_{K(DR)}$ and $I_{K(A)}$ in a voltage-independent manner, the mechanism by which it affects hippocampal potassium channels is the same as that of BPP. But, BCP inhibited $I_{K(DR)}$ and $I_{K(A)}$ in a voltage-dependent manner, so the mechanism by which it affects hippocampal potassium channels is possibly the electrostatic interactions between it and potassium channel proteins.

Our results support the proposition that the action of AChE inhibitors may be related to potassium channels (Harvey and Rowan, 1990). The IC_{50} value of BCP towards $I_{K(DR)}$ and $I_{K(A)}$ (7.13 and 0.55 μM, respectively) is slightly higher than that of them towards AChE on electric eel (0.30 μM). It indicates that the compound appears to be more sensitive to AChE than to these two kinds of currents and AChE could be major action site of them. However, potassium channels might still be other new targets for AChE inhibitors besides AChE (Du et al., 2006). It is a pity that the IC_{50} value of BPP towards AChE on electric eel is slightly higher than that of it towards $I_{K(DR)}$ and $I_{K(A)}$. So, further studies involving other pharmacological compounds structurally related to the central pyridazine are needed to understand the role of various groups and structure–activity relationship of AChE inhibitors in the blockade of AChE on electric eel and the potassium current. Also, it would be more significant, once research targets are expanded to other mammalian neurons, and then these compounds can be applied in clinical study.

Conflict of interest statement

We, Huizhi Du, Miaoyu Li and Pin Yang, declare that we have no proprietary, financial, professional or other personal interest of any nature or kind in any product, service and/or company that could be construed as influencing the position presented in, or the review of, the manuscript entitled, “Effects of 3-benzidino-6-phenylpyridazine, as an acetylcholinesterase inhibitor, on outward potassium current in acutely isolated rat hippocampal pyramidal neurons”.

Acknowledgments

This work was supported by National Nature Science Foundation of China (Grant No. 20637010) and Science Foundation for Youth of Shanxi University (Grant No. 2006003).

References

Benzi, G., Moretti, A., 1998. Is there a rationale for the use of acetylcholinesterase inhibitors in the therapy of Alzheimer's disease? Eur. J. Pharmacol. 346, 1–13.
Bortner, C.D., Hughes Jr., F.M., Cidlowski, J.A., 1997. A primary role for K^+ and Na^+ efflux in the activation of apoptosis. J. Biol. Chem. 272, 32436–32442.
Calavresi, P., Pisani, A., Mercuri, N.B., Bernardi, G., 1995. On the mechanisms underlying hypoxia-induced membrane depolarization in striatal neurons. Brain 118, 1027–1038.
Chen, S.G., Zhou, R.Q., 2001. Enzymology. Fudan University Press, China.
Contreras, J.M., Rival, Y.M., Chayer, S., Bourguignon, J.J., Wermuth, C.G., 1999. Aminopyridazines as acetylcholinesterase inhibitors. J. Med. Chem. 42, 730–741.
Du, H.Z., Zhang, C.F., Li, M.Y., Yang, P., 2006. 3-Benzidino-6 (4-chlorophenyl) pyridazine blocks delayed rectifier and transient outward potassium current in acutely isolated rat hippocampal pyramidal neurons. Neurosci. Lett. 402, 159–163.
Ellman, G.L., Courtney, D., Andres Jr., V., Featherstone, R.M., 1961. A new rapid colorimetric determination of acetylcholineterase activity. Biochem. Pharmacol. 7, 88–95.
Gao, B.X., Ziskind-Conhaim, L., 1998. Development of ionic currents underlying changes in action potential waveforms in rat spinal motoneurons. J. Neurophysiol. 80, 3047–3061.
Garattini, S., Forloni, G.L., Tirelli, S., Ladinsky, H., Consolo, S., 1984. Neurochemical effects of minaprine, a novel psychotropic drug, on the central cholinergic system of the rat. Psychopharmacology 82, 210–214.
Hajimohammadreza, I., Brammer, M.J., Eagger, S., Bruns, A., Levy, R., 1990. Platelet and erythrocyte membrane charges in Alzheimer's disease. Biochim. Biophys. Acta 1025, 208–214.
Harel, M., Schalk, I., Ehret-Sabatier, L., Bouet, F., Goeldner, M., Hirth, C., Axelsen, P.H., Silman, I., Sussman, J.L., 1993. Quaternary ligand binding to aromatic residues in the active site gorge of acetylcholinesterase. Proc. Natl. Acad. Sci. U.S.A. 90, 9031–9035.
Harvey, A.L., Rowan, E.G., 1990. Effects of tacrine, aminopyridines, and physostigmine on acetylcholinesterase, acetylcholine release, and potassium currents. Adv. Neurol. 51, 227–233.
Kamal, M.A., Greig, N.H., Alhomida, A.S., Al-Jafari, A.A., 2000. Kinetics of human acetylcholineterase inhibition by the novel experimental Alzheimer therapeutic agent. Tolserine Biochem. Pharmacol. 60, 561–570.
Kraliz, D., Singh, S., 1997. Selective blockade of the delayed rectifier potassium current by tacrine in Drosophila. J. Neurobiol. 32, 1–10.
Landifield, P.W., Pilter, T.A., 1984. Prolonged Ca^{2+}-dependent after hyperpolarizations in hippocampal neurons of aged rats. Science 226, 1089–1095.
Martina, M., Schultz, J.H., Ehmke, H., Monyer, H., Jones, P., 1998. Functional and molecular differences between voltage-gated K^+ channels of fast-spiking interneurons and pyramidal neurons of rat hippocampus. J. Neurosci. 18, 8111–8125.
Mega, M.S., 2000. The cholinergic deficit in Alzheimer's disease: impact on cognition, behaviour and function. Int. J. Neuropsychopharmacol. 3, 3–12.
Müller, W., Bittner, K., 2002. Differential oxidative modulation of voltage-dependent K^+ currents in rat hippocampal neurons. J. Neurophysiol. 87, 2990–2995.
Müller, W., Misgeld, U., 1990. Inhibitory role of dentate hilus neurons in guinea pig hippocampal slice. J. Neurophysiol. 64, 46–56.
Müller, W., Misgeld, U., 1991. Picrotoxin- and 4-aminopyridineinduced activity in hilar neurons in the guinea pig hippocampal slice. J. Neurophysiol. 65, 141–147.
Pan, Y.P., Xu, X.H., Wang, X.L., 2002. Galantamine blocks delayed rectifier, but not transient outward potassium current in rat dissociated hippocampal pyramidal neurons. Neurosci. Lett. 336, 37–40.

Power, J.M., Oh, M.M., Disterhoft, J.F., 2001. Metrifonate decreases sIAHP in CA1 pyramidal neurons in vitro. J. Neurophysiol. 85, 319–322.
Puglisi-Allegra, S., Cabib, S., Cestari, V., Castellano, C., 1994. Post-training minaprine enhances memory storage in mice: involvement of D1 and D2 dopamine receptors. Psychopharmacology 113, 476–480.
Rogawski, M.A., 1987. Tetrahydroaminoacridine blocks voltage-dependent ion channels in hippocampal neurons. Eur. J. Pharmacol. 142, 169–172.
Sansone, M., Battaglia, M., Vetulani, J., 1995. Minaprine, but not oxiracetam, prevents desipramine-induced impairment of avoidance learning in mice. Pol. J. Pharmacol. 47, 69–73.
Segal, M., Barker, J.L., 1986. Ca^{2+} and Ca^{2+}-dependent K^+ conductances. J. Neurophysiol. 55, 751–766.
Storm, J.F., 1990. Potassium currents in hippocampal pyramidal cells. Prog. Brain Res. 83, 161–187.
Sugimoto, H., 1999. Structure–activity relationships of acetylcholinesterase inhibitors: donepezil hydrochloride for the treatment of Alzheimer's disease. Pure Appl. Chem. 71, 2031–2037.
Sun, X.D., Mo, Z.L., Taylor, B.M., Epps, D.E., 2003. A slowly formed transient conformer of $A\beta^{1-40}$ is toxic to inward channels of dissociated hippocampal and cortical neurons of rats. Neurobiol. Dis. 14, 567–578.
Sussman, J.L., Harel, M., Frolow, F., Oefner, C., Goldman, A., Toker, L., Silman, I., 1991. Atomic structure of acetylcholinesterasefrom *Torpedo californica*: a prototypic acetylcholine-binding protein. Science 253, 872–879.
Tariot, P.N., 1994. Alzheimer's disease: an overview. Alzheimer Dis. Assoc. Dis. 8, S4–S11.
Taylor, C.P., Meldrum, B.S., 1995. Na^+ channels as targets for neuroprotective drugs. Trends Pharmacol. Sci. 16, 309–316.
Worms, P., Kan, J.P., Steinberg, R., Terranova, J.P., Perio, A., Biziere, K., 1989. Cholinomimetic activities of minaprine. Naunyn Schmiedebergs Arch. Pharmacol. 3401, 411–418.
Yamamoto, Y., Ishihara, Y., Kuntz, I.D., 1994. Docking analysis of a series of benzylamino acetylcholinesterase inhibitors with a phthalimide, benzoyl, or indanone moiety. J. Med. Chem. 37, 3141–3153.
Yu, S.P., Farhangrazi, Z.S., Ying, H.S., Yeh, C.H., Choi, D.W., 1998. Enhancement of outward potassium current may participate in β-amyloid peptide-induced cortical neuronal death. Neurobiol. Dis. 5, 81–88.
Zhang, C.F., Yang, P., 2006. Zinc-induced aggregation of Aβ (10–21) potentiates its action on voltage-gated potassium channel. Biochem. Biophys. Res. Commun. 345, 43–49.
Zhang, W., Jin, H.W., Xu, S.F., Qu, L.T., Wang, X.L., 2004. Inhibition of tacrine on delayed rectifier and transient outward potassium currents in cultured rat hippocampal neurons. Acta Pharm. Sin. 39, 93–96.
Zhong, C.B., Zhang, W., Wang, X.L., 2002. Effects of donepezil on the delayed rectifier-like potassium current in pyramidal neurons of rat hippocampus and neocortex. Acta Pharm. Sin. 37, 415–418.